Supporting Information

Krishnaswamy et al. 10.1073/pnas.1501554112

SI Materials and Methods

Generation of Cas9 mRNA and Guide RNAs. To generate Cas9 mRNA, the pCDNA3CAS9HA2XNLS plasmid was linearized with XbaI, phenol/chloroform-extracted, and then used as the template for in vitro transcription (IVT) using the mMESSAGE mMACHINE T7 ULTRA Kit (Life Technologies). To generate guide RNAs (gRNAs), single-stranded DNA oligos were used as templates. Sequences of oligos are shown below (bold sequence represents homology to *Dock8* intronic sequences).

5′ gRNA **CACTGGAAACATGGGCACCA**GTTTTAGAGCTAGAAATAGCAAGTTAAAATAAGGCTAGTCCGTTATCAACTTGAAAAAGTGGCACCGAGTCGGTGCTTTTTT

3′ gRNA **CATTCTAGCTGAGTCCTGTG**GTTTTAGAGCTAGAAATAGCAAGTTAAAATAAGGCTAGTCCGTTATCAACTTGAAAAAGTGGCACCGAGTCGGTGCTTTTTT

A T7 promoter was added to each gRNA template by PCR amplification using the following primers.

5′ forward (F) Gaaattaatacgactcactatagggaga**CACTGGAAACATGGGCACCA**GTTTTAGAGC

5′ reverse (R) AAAAAAGCACCGACTCGGTG

3′ F Gaaattaatacgactcactatagggaga**CATTCTAGCTGAGTCCTGTG**GTTTTAGAGC

3′ R AAAAAAGCACCGACTCGGTG

The T7-gRNA PCR products were column-purified and used as the template for IVT using the MEGAshortscript T7 Kit (Life Technologies). Cas9 mRNA and the gRNAs were purified using the MEGAclear Kit (Life Technologies) and eluted in RNase-free water.

One-Cell Embryo Injection. Superovulated female C57BL/6 mice (4-wk-old) were mated to C57BL/6 stud males, and fertilized embryos were collected from oviducts. Cas9 mRNAs (100 ng/μL) and gRNA (each 50 ng/μL) were resuspended in injection buffer (5 mM Tris·Cl, pH 7.4; 0.1 mM EDTA, pH 8.0), and injected into the cytoplasm of fertilized eggs. Injected zygotes were transferred into the uterus of pseudopregnant females. Resulting pups were genotyped by PCR and Sanger sequencing to confirm deletion of exons 10–14 using the following primers: forward 5′-TTGGTGGTGAGCTTTGGGAG-3′; reverse 5′-TCTGTCATGATGGGCCTTGG-3′.

Antibodies. CD11c (N418), I-A/I-E (M5/114.15.2), TCRβ (H57-597), B220 (RA3-6B2), CD23 (B3B4), CD21/35 (7E9), IgD (11-26c-2a), GR1 (RB6-8C5), CD11b (M1/70), Vα2 (B20.1), CD45.1 (A20), CD4 (GK1.5), CD45.2 (104), CD3 (145-2C11), and IL-5 (TRFK5) antibodies and Brilliant Violet 421 streptavidin were purchased from BioLegend. IgM (II/41) and I-A^k (11-5.2) were purchased from BD Biosciences.

BMDC Culture. Bone marrow-derived dendritic cells (BMDCs) were cultured as described previously (1). Briefly, bone marrow cells were cultured on non–tissue culture-treated plates for 7 d in complete RPMI supplemented with 20 ng/mL recombinant GM-CSF (PeproTech). On day 8, BMDCs were gently flushed, transferred to tissue culture-treated plates, and activated with LPS (100 ng/mL or 1 μg/mL). LPS-treated BMDCs were further stimulated with CCL19 (100 ng/mL) as indicated.

Marginal Zone B-Cell Analyses. Single-cell suspensions of splenocytes were stained for marginal zone B cells. Marginal zone B cells were identified as $CD11b^{-}GR\text{-}1^{-}$ $B220^{+}CD21^{+}CD23^{-}$ cells.

Relative Gene Expression Analyses. RNA isolation and real-time PCR analysis were performed as previously described (2). Briefly, RNA was isolated from BMDCs using TRIzol (Invitrogen). cDNA was prepared using Oligo(dT) (Sigma), dNTPs (Lamda Biotech), and the SMART MMLV Reverse Transcriptase Kit (Clontech Laboratories). Real-time PCR for *Dock8* was performed using PerfeCTa SYBR Green FastMix, Low ROX (Quanta Biosciences), whereas for *Gdpd3*, commercially available primer/probe sets were purchased (Applied Biosystems). cDNA expression was analyzed by the $\Delta\Delta C_t$ (change in cycle threshold) method (3), and results were normalized to ΔC_t values of Hprt obtained in parallel reactions during each cycle and then expressed relative to control samples (3). The following primers were used: *Dock8*; forward 5′-GTCACCTCGGAGATAGCAGC-3′, reverse 5′-GAACACGAAGCCTCTGTCCA-3′; *HPRT*; forward 5′-CTGGTGAAAAGGACCTCTCG-3′, reverse 5′-TGAAGTACTCATTATAGTCAAGGGCA-3′ (Sigma). Primer/probe sets purchased included *Gdpd3* Mm00470322_m1 and *Hprt* Mm00446968_m1 (Applied Biosystems).

Western Blot Analyses. Day 8 BMDCs were collected and lysed using RIPA buffer (150 mM sodium chloride, 1.0% Nonidet P-40 or Triton X-100, 0.5% sodium deoxycholate, 0.1% SDS, and 50 mM Tris, pH 8.0) containing 1× phosphatase and protease inhibitor mixture (Roche). Total protein was quantified using Precision Red Advanced Protein Assay Reagent (Cytoskeleton). Lysates were mixed with 5× Laemmli buffer for SDS/PAGE and Western blot analysis. Antibodies against DOCK8 (Clontech Laboratories) and actin-HRP (Santa Cruz Biotechnology) were used for protein detection. Secondary antibodies were bought from Jackson ImmunoResearch.

CDC42 Pull-Down Assay. Purified CDC42-GST (5 μg; Cytoskeleton) was loaded on glutathione beads. BMDC lysates containing either 20 mM EDTA (E buffer) or 100 mM $MgCl_2$ and 200 μM GTPγS (M buffer) were incubated with CDC42-GST–loaded beads for 4 h at 4 °C (continuous mixing). Beads were then washed three times using cell lysis buffer and boiled for 10 min at 100 °C in 2× Laemmli buffer. Samples were centrifuged at 15,000 × *g* and supernatants were loaded on SDS/PAGE gels followed by Western blot analysis for DOCK8.

Quantitative Proteomics.

Cell lysis, filter-aided sample preparation, and iTRAQ 4-plex labeling. In two biological replicates, BMDCs from wild-type and NLRP10-deficient mice were stimulated or not for 16 h with 100 ng/mL LPS. Cell pellets corresponding to 5×10^6 cells were resolubilized in 100 μL 50 mM Hepes buffer (pH 8.0), 2% (wt/vol) SDS, 1 mM PMSF, and protease inhibitor mixture (Sigma-Aldrich Chemie). DNA was sheared by sonication for 80 s using a Covaris S2x ultrasonicator applying a 10% duty cycle with 200 cycles per burst at an intensity of 5. Crude cell lysate was cleared by centrifugation at 16,000 × *g* for 10 min at 20 °C and the supernatant was transferred to a new Eppendorf tube. Protein concentration was determined with the bicinchoninic protein assay (Pierce Biotechnology, Thermo Fisher Scientific). Total protein (100 μg in duplicates) was processed by an adapted filter-aided sample preparation (FASP) method (4, 5). Briefly, proteins were reduced with 100 mM DTT, and SDS was exchanged with 8 M urea in 100 mM

Tris·HCl buffer (pH 8.0). Reduced disulfide bonds were alkylated with 50 mM iodoacetamide, and samples were washed with 50 mM triethylammonium bicarbonate buffer (pH 8.2). Proteins were digested overnight with porcine trypsin (Promega) in an enzyme-to-protein ratio of 1:100 (wt/wt). Tryptic peptides were concentrated and purified by reversed-phase (RP) C18 solid-phase extraction (SPE; MacroSpin columns, 30–300 μg capacity; The Nest Group) and derivatized with amine-reactive isobaric iTRAQ 4-plex mass tag reagents according to the instructions provided by the manufacturer (Applied Biosystems). Samples were labeled as follows: iTRAQ-label 114, untreated wild-type dendritic cells; iTRAQ-label 115, LPS-treated wild-type dendritic cells; iTRAQ-label 116, untreated NLRP10 knockout dendritic cells; and iTRAQ-label 117, LPS-treated NLRP10 knockout dendritic cells.

Offline fractionation via RP-HPLC and online nano-RP-LC-MSMS. Pooled samples (iTRAQ 114–118) were concentrated and purified by RP C18 SPE and separated on a Phenomenex column (150 × 2.0 mm Gemini NX-C18, 3 μm, 110 Å) by reversed-phase liquid chromatography using an Agilent 1200 series HPLC with UV detection at 214 nm. HPLC solvent A consisted of 20 mM ammonium formate (pH 10) in 5% (vol/vol) acetonitrile, and solvent B consisted of 20 mM ammonium formate (pH 10) in 90% (vol/vol) acetonitrile. Peptides were separated at a flow rate of 100 μL/min and eluted from the column with a nonlinear gradient ranging from 0 to 100% solvent B. Seventy-two time-based fractions were collected, acidified with 5% (vol/vol) formic acid, and pooled into 50 HPLC vials based on the UV trace. The solvent was evaporated in a vacuum concentrator at 45 °C and reconstituted in 5% (vol/vol) formic acid. Mass spectrometry was performed on a hybrid linear trap quadrupole (LTQ) Orbitrap Velos mass spectrometer (Thermo Fisher Scientific) using Xcalibur (v2.1.0.1140) coupled to an Agilent 1200 HPLC nanoflow system (dual-pump system with trapping column and analytical column) via a nanoelectrospray ion source using liquid junction (Proxeon). Solvents for LC/MS separation of the digested, labeled samples were as follows: solvent A consisted of 0.4% formic acid in water, and solvent B consisted of 0.4% formic acid in 70% methanol and 20% isopropanol. Peptide samples were loaded onto a trap column (Zorbax 300SB-C18, 5 μm, 5 × 0.3 mm; Agilent Biotechnologies) at a flow rate of 45 μL/min. TFA (0.1%) was used for loading and washing the precolumn. After washing, the peptides were eluted by backflushing onto a 16-cm fused silica analytical column with an inner diameter of 50 μm packed with C18 reversed-phase material (ReproSil-Pur 120 C18-AQ, 3 μm; Dr. Maisch). The peptides were eluted from the analytical column with a 27-min gradient ranging from 3% to 30% solvent B, followed by a 25-min gradient from 30% to 70% solvent B and, finally, a 7-min gradient from 70% to 100% solvent B at a constant flow rate of 100 nL/min (6). The analyses were performed in a data-dependent acquisition mode using a top 10 higher-energy collisional dissociation method. Dynamic exclusion for selected ions was 60 s. The siloxane at m/z 445.12003 was used as a recalibration lock mass (7). Automatic gain control was used to prevent overfilling of the ion traps with target ion values of 10^6 and 10^5 for full Fourier transform mass spectrometer (FTMS) and MS^2 scans, respectively. Maximal ion accumulation time was 200 ms for MS^2 scans. Full FTMS and MS^2 scans were performed at a resolution of 30,000 and 7,500, respectively. The threshold for switching from MS to MS^2 was 5,000 counts, and normalized collision energy was 40%.

Data processing. The acquired raw MS data files were processed with msconvert (ProteoWizard Library v2.1.2708) and converted into Mascot generic format (mgf) files. Peptide identification was performed by searching the resultant peak lists against the SwissProt mouse database v2012.05_20120529 [24,502 sequences including isoforms obtained from varsplic.pl (8) and appended known contaminants] with the search engines Mascot (v2.3.02; Matrix Science) and Phenyx (v2.5.14; GeneBio) (9). Submission to the search engines was via a Perl script that performs an initial search with relatively broad mass tolerances (Mascot only) on both the precursor and fragment ions (±10 ppm and ±0.6 Da, respectively). High-confidence peptide identifications were used to recalibrate all precursors and fragment ion masses before a second search with narrower mass tolerances (±4 ppm and ±0.025 Da). Trypsin was chosen for cleavage specificity with the maximum of one miscleavage site allowed. Carbamidomethylated cysteine residues and N-terminal and lysine-modified iTRAQ 4-plex were chosen as fixed modifications. Oxidized methionine was chosen as the only variable modification. To validate the proteins, Mascot and Phenyx output files were processed by internally developed parsers. Proteins with ≥2 unique peptides above a score T1, or with a single peptide above a score T2, were selected as unambiguous identifications. Additional peptides for these validated proteins with score >T3 were also accepted. For Mascot and Phenyx, T1, T2, and T3 peptide scores were equal to 12, 45, and 10 and 5.5, 9.5, and 3.5, respectively (P value $<10^{-3}$). The validated proteins retrieved by the two algorithms were merged, and any spectral conflicts were discarded and grouped according to shared peptides. A false positive detection rate (FDR) of <1% and <0.1% was determined for proteins and peptides, respectively, by applying the same procedure against a reversed database. Relative quantitation of proteins was calculated using isobar (10), which corrected for isotopic impurities of the iTRAQ 4-plex reagents and normalized median iTRAQ channel intensities. Ratios were calculated based on unique peptides, excluding shared peptides. In addition, contaminating human proteins and keratin species were removed from the final dataset. Mean ratios of NLRP10 knockout over wild type (ko/wt) under unstimulated and LPS-stimulated conditions were calculated for the intersection of 5,127 individual proteins of the two biological replicates. P values from two independent experiments were combined using Fisher's method.

Whole-Exome Sequencing. Sequencing was performed by the Scientific Services at The Jackson Laboratory. One microgram of DNA was fragmented using a Covaris E220 to a range of sizes centered on 300 bp. The precapture library was prepared using the NEBNext DNA Library Prep Master Mix Set for Illumina (New England BioLabs) including a bead-based size selection for inserts with an average size of 300 bp and 18 cycles of PCR. The resulting precapture library was hybridized to the Roche NimbleGen Mouse Exome capture probe set according to the manufacturer's instructions. The final captured libraries were amplified by 12 cycles of PCR using HiFi HotStart ReadyMix (Kapa Biosystems). The resulting sequencing libraries were quantified by quantitative PCR, pooled, and sequenced on an Illumina HiSeq 2500.

Samples were subjected to quality control using *NGSQCtoolkit* v2.3, and reads with base qualities ≥30 over 70% of read length were used in the downstream analysis (11). High-quality reads were mapped to the mouse genome (build-mm10) using *BWA v0.5.10-tpx* (12) at default parameters. The resulting alignment was sorted by coordinates and further converted to binary alignment map (BAM) format by the *Picard v1.95-SortSam* utility (broadinstitute.github.io/picard/). The *Picard-MarkDuplicates* module was used to remove duplicates from the data. Afterward, the *Genome Analysis Toolkit* (GATK) v3.1-1 (13, 14) module *IndelRealigner* was used to preprocess the alignments. The target capture efficiency metric was determined using *Picard-HsMetrics*. The realigned and recalibrated bam alignment file was used as an input to *GATK-HaplotypeCaller* at parameters -stand_call_conf 50.0, -stand_emit_conf 30.0, and -dcov 250, and variants calls were restricted to the target region. Finally, raw variant calls were soft-filtered using *GATK VariantFiltration* and annotated by *snpEff* v2.0.5 (15), and the highest impact variant was reported by *GATK VariantAnnotator*.

SNP Analyses and Hierarchical Clustering. Using the mouse phenome database (phenome.jax.org/SNP), we initially queried the Sanger1 dataset for all informative (i.e., variation present in at least one strain) single-nucleotide polymorphisms (SNPs) in 19 inbred strains of mice, including the BALB/cJ, C3H/HeJ, C57BL/6J, and CBA/J strains used in the present study. We found 6,549 informative SNPs (Dataset S1) and performed hierarchical clustering analyses of the SNPs as described previously (16). Hamming distance between each strain pair was calculated as the number of polymorphic nucleotides within *Dock8* where the strains were different. We partitioned the strains into haplotype groups using hierarchical clustering on the distance matrix using Ward's method (stat.ethz.ch/R-manual/R-patched/library/stats/html/hclust.html). All of the strains clustered into one of three major haplotypes (Fig. S5), and the greatest genetic variation was found in the wild-derived strains PWK/PhJ, CAST/EiJ, and SPRET/EiJ. We then queried the haplotypes for nonsynonymous coding SNPs and, among the BALB/cJ, C3H/HeJ, C57BL/6J, and CBA/J strains, one SNP (rs37224966) had a 0.00 SIFT score (sift.jcvi.org/) that is predicted to be deleterious to DOCK8 protein function. This C/T SNP causes an Arg/Trp residue change and was found only in the C3H/HeJ strain.

Asthma Model and Intracellular Cytokine Analysis. Six- to eight-wk-old CBA/J and C3H/HeJ mice were immunized intraperitoneally with OVA (100 μg per mouse) and Alum (1.5 mg per mouse) on day 0 and day 7 followed by airway challenge with OVA (25 μg per mouse intranasal) on days 14, 15, 18, and 19. On day 20, mice were killed and mediastinal LNs were harvested (2). Intracellular cytokine detection was performed as described previously (17). Briefly, single-cell suspensions were restimulated for 5 h with phorbol 12-myristate 13-acetate (50 ng/mL) and ionomycin (1 μg/mL); GolgiStop (1 μL/mL) was added for the last 4 h of stimulation. Surface staining with CD3, CD4, and CD44 antibodies and intracellular cytokine staining with IL-5 antibody were performed using the BD Cytofix/Cytoperm Kit (BD Biosciences) as per the manufacturer's protocol.

Statistical Analyses. For statistical analysis, one-way ANOVA was performed followed by Bonferroni's multiple comparisons test for comparing different groups (GraphPad; Prism).

1. Sixt M, Lämmermann T (2011) In vitro analysis of chemotactic leukocyte migration in 3D environments. *Methods Mol Biol* 769:149–165.
2. Eisenbarth SC, et al. (2012) NLRP10 is a NOD-like receptor essential to initiate adaptive immunity by dendritic cells. *Nature* 484(7395):510–513.
3. Livak KJ, Schmittgen TD (2001) Analysis of relative gene expression data using real-time quantitative PCR and the 2(-Delta Delta C(T)) Method. *Methods* 25(4):402–408.
4. Manza LL, Stamer SL, Ham AJ, Codreanu SG, Liebler DC (2005) Sample preparation and digestion for proteomic analyses using spin filters. *Proteomics* 5(7):1742–1745.
5. Wiśniewski JR, Zougman A, Nagaraj N, Mann M (2009) Universal sample preparation method for proteome analysis. *Nat Methods* 6(5):359–362.
6. Bennett KL, et al. (2011) Proteomic analysis of human cataract aqueous humour: Comparison of one-dimensional gel LCMS with two-dimensional LCMS of unlabelled and iTRAQ®-labelled specimens. *J Proteomics* 74(2):151–166.
7. Olsen JV, et al. (2005) Parts per million mass accuracy on an Orbitrap mass spectrometer via lock mass injection into a C-trap. *Mol Cell Proteomics* 4(12):2010–2021.
8. Kersey P, Hermjakob H, Apweiler R (2000) VARSPLIC: Alternatively-spliced protein sequences derived from SWISS-PROT and TrEMBL. *Bioinformatics* 16(11):1048–1049.
9. Colinge J, Masselot A, Giron M, Dessingy T, Magnin J (2003) OLAV: Towards high-throughput tandem mass spectrometry data identification. *Proteomics* 3(8):1454–1463.
10. Breitwieser FP, et al. (2011) General statistical modeling of data from protein relative expression isobaric tags. *J Proteome Res* 10(6):2758–2766.
11. Patel RK, Jain M (2012) NGS QC Toolkit: A toolkit for quality control of next generation sequencing data. *PLoS ONE* 7(2):e30619.
12. Li H, Durbin R (2009) Fast and accurate short read alignment with Burrows-Wheeler transform. *Bioinformatics* 25(14):1754–1760.
13. DePristo MA, et al. (2011) A framework for variation discovery and genotyping using next-generation DNA sequencing data. *Nat Genet* 43(5):491–498.
14. McKenna A, et al. (2010) The Genome Analysis Toolkit: A MapReduce framework for analyzing next-generation DNA sequencing data. *Genome Res* 20(9):1297–1303.
15. Cingolani P, et al. (2012) A program for annotating and predicting the effects of single nucleotide polymorphisms, SnpEff: SNPs in the genome of *Drosophila melanogaster* strain w1118; iso-2; iso-3. *Fly (Austin)* 6(2):80–92.
16. Cho HY, et al. (2015) Association of Nrf2 polymorphism haplotypes with acute lung injury phenotypes in inbred strains of mice. *Antioxid Redox Signal* 22(4):325–338.
17. Gowthaman U, et al. (2011) Promiscuous peptide of 16 kDa antigen linked to Pam2Cys protects against *Mycobacterium tuberculosis* by evoking enduring memory T-cell response. *J Infect Dis* 204(9):1328–1338.

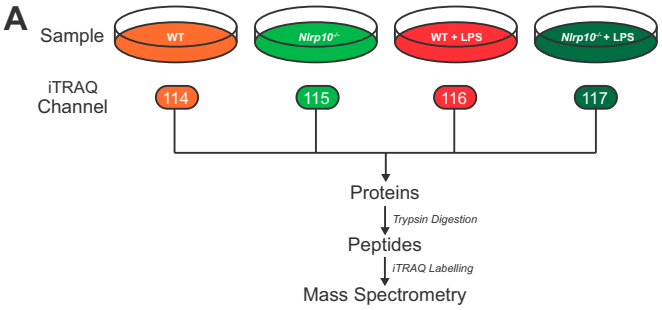

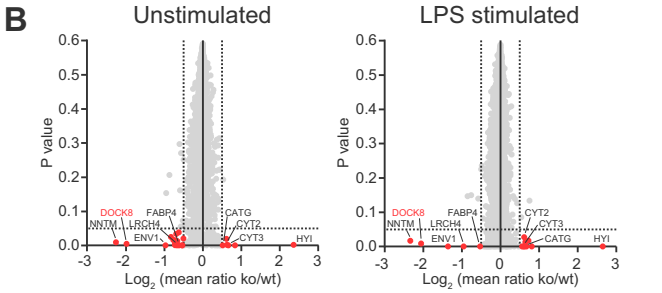

C

Unstimulated

UNIPROT ID	log_2 (mean ratio ko/wt)
NNTM_MOUSE	-2.2615
DOCK8_MOUSE	-1.9856
ENV1_MOUSE	-0.9727
PYGM_MOUSE	-0.8271
BIR1E_MOUSE	-0.7659
CHD9_MOUSE	-0.7248
ZAP70_MOUSE	-0.7218
CXL16_MOUSE	-0.7205
MYH1_MOUSE	-0.6895
LRCH4_MOUSE	-0.6755
MADD_MOUSE	-0.6670
PRKX_MOUSE	-0.6662
IFI44_MOUSE	-0.6233
FABP4_MOUSE	-0.6217
MFGM_MOUSE	-0.5378
ANT3_MOUSE	-0.5301
MINK1_MOUSE	-0.5035
CATG_MOUSE	0.5182
EF1D_MOUSE	0.6145
CYT2_MOUSE	0.6309
CYT3_MOUSE	0.6630
COX7B_MOUSE	0.8380
HYI_MOUSE	2.3621

LPS stimulated

UNIPROT ID	log_2 (mean ratio ko/wt)
NNTM_MOUSE	-2.3375
DOCK8_MOUSE	-2.0538
ENV1_MOUSE	-1.3572
LRCH4_MOUSE	-0.9548
FABP4_MOUSE	-0.5257
PERM_MOUSE	0.5620
PRTN3_MOUSE	0.6004
TSP1_MOUSE	0.6107
CYT2_MOUSE	0.6148
CYT3_MOUSE	0.6251
ELNE_MOUSE	0.6467
CATG_MOUSE	0.6723
THY1_MOUSE	0.7289
PLF4_MOUSE	0.8125
HYI_MOUSE	2.6524

Fig. S1. (*A*) Experimental outline of iTRAQ-based expression proteomics of WT and NLRP10-deficient BMDCs in the presence or absence of LPS. (*B*) Mean log_2-transformed protein ratios (ko/wt) from two biological replicates of unstimulated (*Left*) or LPS-stimulated DCs (*Right*) plotted against their combined *P* values. Red dots indicate proteins that were significantly (combined *P* value <0.05) down- (log_2 of mean ratio <−0.5) or up-regulated (log_2 of mean ratio >0.5). Proteins that meet these criteria under both unstimulated and LPS-stimulated conditions are annotated. (*C*) Tables showing proteins that were either down- (green bars; log_2 of mean ratios <−0.5) or up-regulated in NLRP10-deficient DCs (red bars; log_2 of mean ratios >0.5). (*Left*) Unstimulated. (*Right*) LPS-stimulated DCs. Only proteins with combined *P* values <0.05 from two biological replicates are shown.

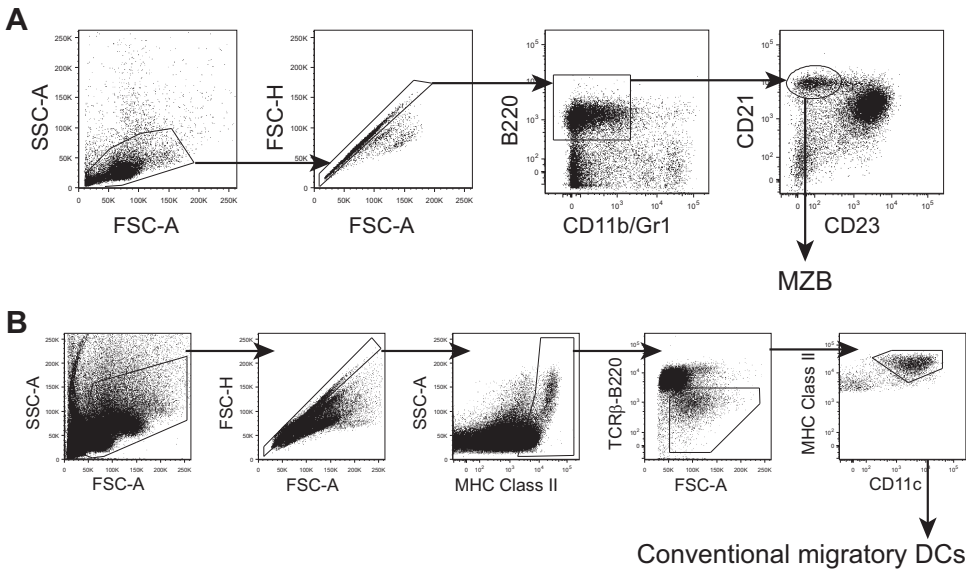

Fig. S2. Gating strategy for (*A*) marginal zone B cells and (*B*) conventional migratory DCs. FSC-A, forward scatter area; FSC-H, forward scatter height; MHC Class II, major histocompatibility complex class II; MZB, marginal zone B cells; SSC-A, side scatter area.

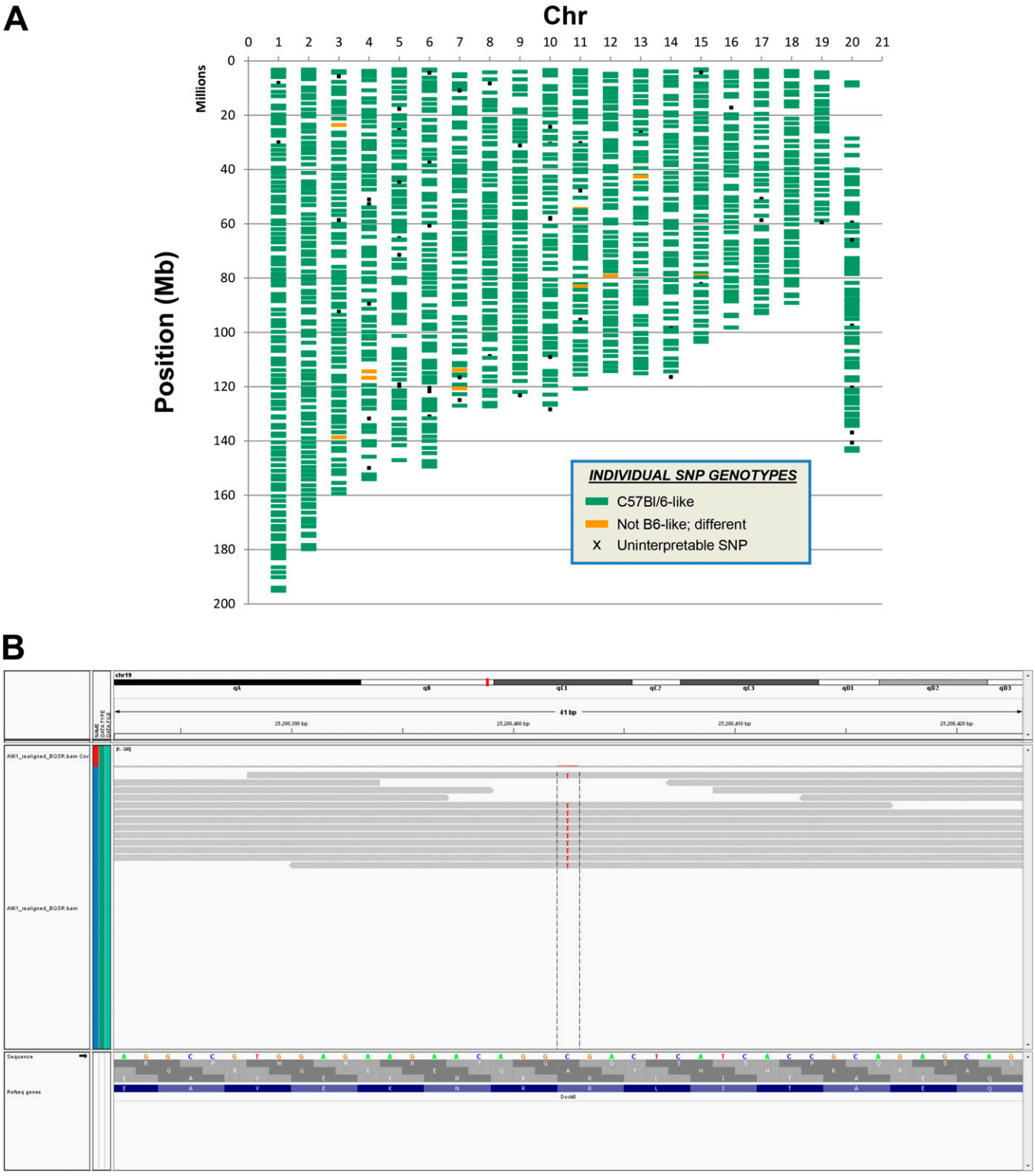

Fig. S3. (*A*) Whole-genome SNP analysis of *Nlrp10*$^{-/-}$ mice versus the reference Jax C57BL/6 genotype as performed by DartMouse (www.dartmouse.org). C57BL/6J-like regions are depicted in green, whereas regions that are not C57BL/6J-like are shown in yellow. (*B*) IGV (Integrated Genome Viewer) view of pair-end sequence data aligned to the mouse genome (mm10) (www.broadinstitute.org/igv/). Chr19 locus 25200402 (*Dock8* region) shows the occurrence of SNP "T" (in red) in all aligned reads (gray bars). Total read depth is 10 at this locus.

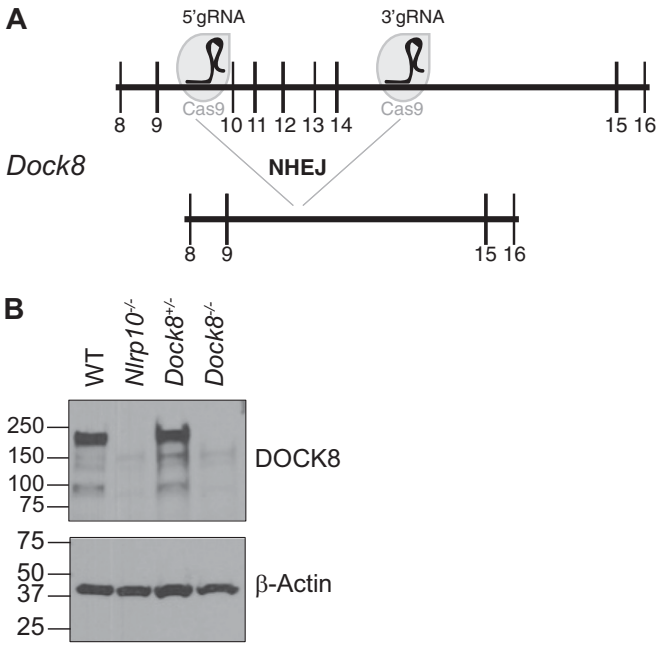

Fig. S4. Deletion of exons 10–14 of the *Dock8* gene results in complete protein loss. (*A*) Targeting details of the deletion of exons 10–14 of *Dock8* using CRISPR/Cas9 genome-editing technology. Guide RNAs were designed against intronic sequences flanking exons 10–14 (see *SI Materials and Methods* for sequences). In vitro transcribed Cas9 mRNA and gRNAs were injected into fertilized oocytes to generate DOCK8 knockout mice as previously described (1). Cas9-mediated double-stranded DNA breaks were resolved by nonhomologous end joining (NHEJ), thereby ablating the intervening sequences containing exons 10–14. Resulting offspring were sequenced to confirm deletion. (*B*) Western blot analysis of DOCK8 from total cell lysates of WT, *Nlrp10*$^{-/-}$ *Dock8*$^{mu/mu}$ (referred to as *Nlrp10*$^{-/-}$), *Dock8*$^{+/-}$, and *Dock8*$^{-/-}$ BMDCs.

1. Wang H, et al. (2013) One-step generation of mice carrying mutations in multiple genes by CRISPR/Cas-mediated genome engineering. *Cell* 153(4):910–918.

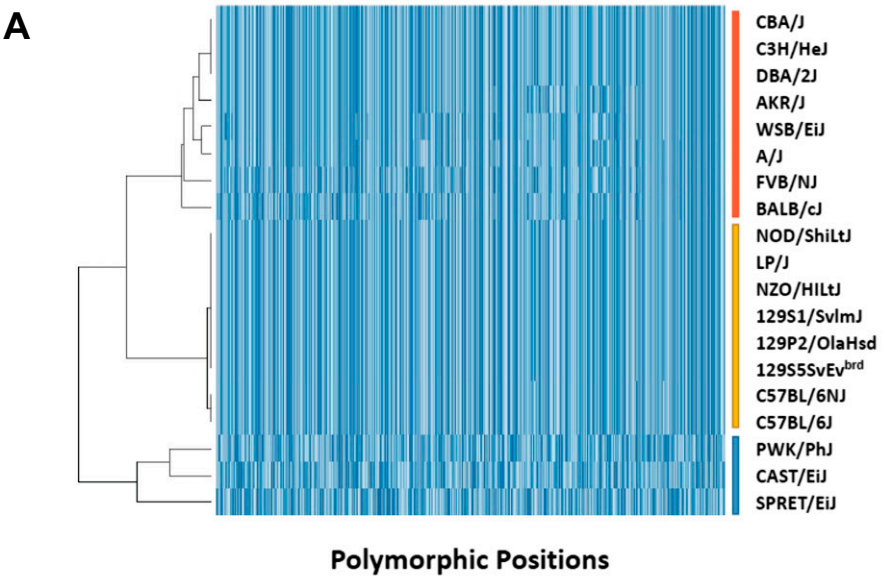

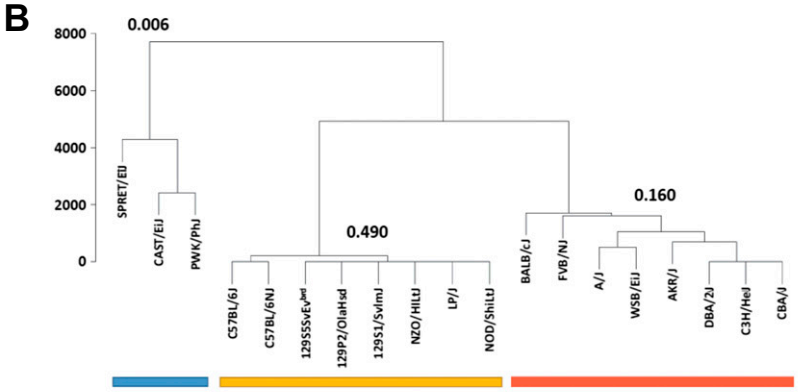

C

Chromosome number	rs ID Number	BP Location	Observed change	Consequence	db SNP annotation	Inbred Strains C57BL/6J	BALB/cJ	C3H/HeJ	CBA/J
19	rs258788308	24999562	A/C/G	U5	U5:Dock8	C	A	C	C
19	rs234349977	24999642	G/T	U5	U5:Dock8	G	T	G	G
19	rs30522591	25095600	A/G	Cn	Cn:Dock8:IV:415	A	A	G	G
19	rs50235883	25132073	C/T	Cn	Cn:Dock8:TI:873	C	C	T	T
19	rs37224966	25154187	C/T	Cn	Cn:Dock8:RW:1094	C	C	T	C
19	rs30323665	25200466	A/G	Cn	Cn:Dock8:RK:2055	G	A	G	G
19	rs31245139	25201862	A/G	U3	U3:Dock8	A	G	A	A
19	rs30452618	25201865	C/G	U3	U3:Dock8	G	C	G	G
19	rs30503342	25201993	A/G	U3	U3:Dock8	A	G	A	A
19	rs30919295	25202261	A/G	U3	U3:Dock8	A	G	A	A
19	rs239025681	25202306	C/T	U3	U3:Dock8	C	C	C	C
19	rs31074572	25202314	A/G	U3	U3:Dock8	A	G	A	A
19	rs31237272	25202368	A/G	U3	U3:Dock8	G	A	G	G

D

CBA/J	CCA-ACG-CTC-ATC-TCC-ATG-**C**GG-CTG-GAA-TTC-CTG-AGG-ATC Pro-Thr-Leu-Ile-Ser-Met-**Arg**-Leu-Glu-Phe-Leu-Arg-Ile
C3H/HeOuJ	CCA-ACG-CTC-ATC-TCC-ATG-**C**GG-CTG-GAA-TTC-CTG-AGG-ATC Pro-Thr-Leu-Ile-Ser-Met-**Arg**-Leu-Glu-Phe-Leu-Arg-Ile
C3HeB/FeJ	CCA-ACG-CTC-ATC-TCC-ATG-**C**GG-CTG-GAA-TTC-CTG-AGG-ATC Pro-Thr-Leu-Ile-Ser-Met-**Arg**-Leu-Glu-Phe-Leu-Arg-Ile

Fig. S5. Genetic variability of *Dock8* across inbred and outbred strains of mice including C3H/HeJ. (*A*) Heat map of all *Dock8* SNPs among 19 inbred strains of mice. Blue, yellow, and red rectangles correspond to the three major *Dock8* haplotypes. (*B*) Hierarchical clustering of 19 inbred strains of mice based on 6,549 SNPs found in the Sanger1 database. Numbers represent the uncertainty in genotype changes after clustering (Φ), where Φ = 1 − cluster entropy/crude entropy. If, after clustering, all strains in the cluster have the same genotype, then Φ = 1. If the genotype distribution within the cluster is as variable as the genotype distribution across all strains, then Φ = 0. (*C*) Truncated haplotype structure of *Dock8* with nonsynonymous coding (Cn) and 3′ untranslated (U3) and 5′ untranslated (U5) SNPs in C57BL/6J, BALB/cJ, C3H/HeJ, and CBA/J strains of mice. The rs37224966 C/T SNP (orange font) is predicted to cause deleterious effects in the Dock8 protein (see text). (*D*) Sequencing of the affected region of the *Dock8* gene in C3H/HeJ mice in closely related strains, CBA/J, C3H/HeOuJ, and C3HeB/FeJ, confirmed a wild-type sequence in all three of these strains. Nucleotide and amino acid residue in bold indicate the position of Dock8 mutation in exon 27 of C3H/HeJ mice.

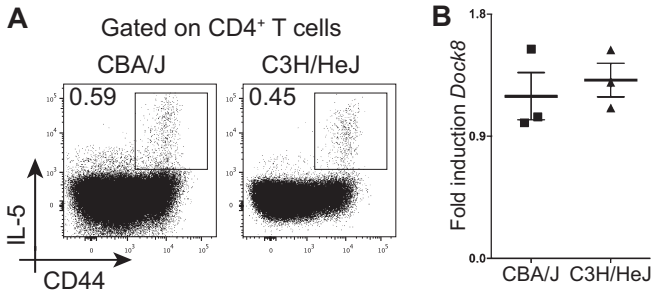

Fig. S6. *Dock8* point mutation in C3H/HeJ mice does not significantly impair in vivo T-cell activation or *Dock8* mRNA expression in BMDCs. (*A*) Intracellular cytokine staining for IL-5 in T cells from mediastinal LNs of CBA/J and C3H/HeJ mice sensitized using the asthma model. (*B*) Semiquantitative PCR of *Dock8* in unstimulated BMDCs from CBA/J versus C3H/HeJ mice.

Table S1. Homozygous high-impact genetic changes in the *Nlrp10*$^{-/-}$ strain identified by whole-exome sequencing

Chr	Position	Gene ID	Gene	Mutation	Altered mRNA	Altered protein	Function
4	118360337	*Hyi*	Hydroxypyruvate isomerase homolog	Indel: splice-site acceptor	No	Yes ↑	Putative hydropyruvate isomerase
5	124624334	*Tctn2*	Tectonic family member 2	Indel: splice-site acceptor	No	NA	Type I membrane protein in tectonic family
7	128671134	*Inpp5f*	Inositol polyphosphate-5-phosphatase f	Indel: frameshift	No	No	Inositol 5-phosphatase
11	78400940	*Slc13a2os*	Slc13a member 2, opposite strand	Indel: frameshift	NA	NA	Noncoding RNA
15	9100143	*Nadk2*	NAD kinase 2	Indel: frameshift	NA	No	Mitochondrial NAD kinase
19	25200402	*Dock8*	Dedicator of cytokinesis 8	SNP: nonsense	Yes ↓	Yes ↓	Guanine nucleotide exchange factor

Variants present in dbSNPv137 [mm10] and variants without the "PASS" in the filter column of the variant call file were excluded. Chr, chromosome location of gene; Position on chromosome of the indicated gene; Gene ID, gene name; mutation shows type of change: Indel, insertion/deletion with genetic effect, or SNP, single nucleotide polymorphism with genetic effect; Altered mRNA cross-references whether separate data indicated altered levels of transcripts (NA, not assayed); Altered protein indicates whether the identified genes were also found to be altered in the proteomics screen from Fig. 1; Function predicted of indicated gene.

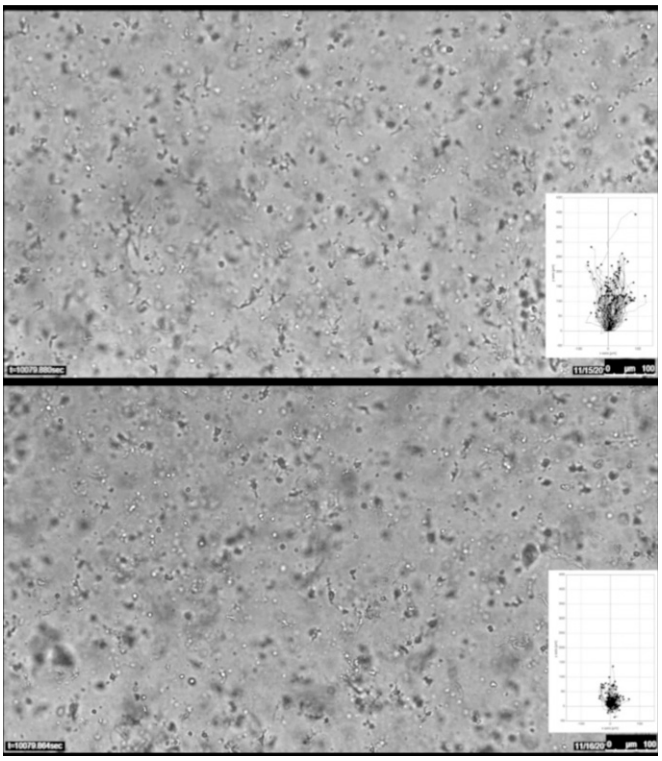

Movie S1. Migration of LPS-stimulated WT (upper frames) and *Nlrp10*$^{-/-}$ (lower frames) BMDCs in a 3D collagen matrix toward a source of CCL19. Collagen gel (1.6 mg/mL); CCL19 source (250 ng/mL); time-lapse microscopy over 4 h at 2 frames per min; total magnification 100×.

Movie S1

Other Supporting Information Files

Dataset S1 (XLSX)